Assessment of Onshore Wind Turbine Fatigue Damage Subjected to Tropical Cyclone

C. Sheng
Post-Doctoral Associate, Department of Civil and Environmental Engineering, University of Western Ontario, London, Ontario, Canada. Email: csheng9@uwo.ca

H. P. Hong
Professor, Department of Civil and Environmental Engineering, University of Western Ontario, London, Ontario, Canada. Email: hhong@uwo.ca

ABSTRACT: Tropical cyclones (TCs) affect structures and infrastructure systems. They can cause low-cycle high amplitude stress for onshore and offshore structures, such as wind turbines (WTs). This study aims to evaluate the impact of TCs on the accumulated fatigue damage for onshore WTs located along the southeast coastal region of mainland China. The analysis is carried out using a simulation-based framework, which includes the use of simulated stochastic TC tracks, TC wind field model, and dynamic responses of onshore WT. In particular, the National Renewable Energy Laboratory (NREL) 5 MW WT placed at two locations in the coastal region of mainland China is considered. For the example WT, analysis results indicate that fatigue damage for the tower structure could be more severe than that for the blade; fatigue damage is also site-dependent since the TC wind hazard is geographically varying. The lifetime fatigue damage can be as much as 9% of the designed capacity for the tower provided that the classic Miner's rule is assumed.

1. INTRODUCTION

Wind turbines (WTs) that are located in tropical cyclone (TC) hazard-prone regions could experience severe TC wind loading. TC is a large-scale weather system characterized by strong winds. Structural damage and failure of WTs due to TCs have been reported in the literature. The observed damages include blade fracture, tower bucking, and foundation overturning (Li et al. 2013). The damage survey reported by Chen et al. (2015) indicated that TC winds caused failures of WT structural as well as mechanical systems.

The assessment of reliability and risk level for WTs subjected to TCs was given by Rose et al. (2012), Hallowell et al. (2018), Sheng and Hong (2021), and Hong and Sheng (2022). These studies were focused on the ultimate limit states. Since a TC event could impact a site with strong winds for several hours, such long-duration winds could cause low-cycle high-amplitude stresses resulting in fatigue damage (Amirinia and Jung 2017; Chen et al. 2021, 2022). The analysis by Chen et al. (2022) indicated that TCs can reduce the fatigue design capacity for WT by up to about 20%. However, in these mentioned studies, simplifying assumptions on the TC hazard, in terms of TC track and TC wind field modeling were made for the TC-induced fatigue damage assessment.

The main objective of this study is to assemble an overall framework to assess the TC-induced fatigue damage for WTs and to use the framework to evaluate the accumulated fatigue damage for WTs that are placed at onshore locations in the coastal regions in mainland China. The framework takes into account the stochastic TC full track model, TC wind field model, and WT responses subjected to TC wind hazard. Numerical evaluation of the accumulated fatigue damage is carried out by considering the National Renewable Energy Laboratory (NREL) 5 MW onshore WT (Jonkman et al. 2009) as the example WT and the 100,000-year simulated TC activities.

2. AN INTEGRATED ASSESSMENT FRAMEWORK

2.1. Overview

The adopted analysis framework for the fatigue damage assessment due to TC events consists of three components: site-specific TC wind hazard modeling, wind turbine response modeling, and fatigue damage accumulation assessment. The required analysis within each component is shown in Figure 1. The adopted framework is similar to that presented by Sheng and Hong (2020) and Hong and Sheng (2022) for the reliability analysis of WTs subjected to TC hazard by considering the ultimate limit state function.

As shown in Figure 1, the first component provides the probabilistic assessment of the TC wind hazard, while the second component gives the fragility curve which requires extensive structural analysis that could take into account the uncertainty in structural material properties and geometrical variables. The last component combines the results from the first two components to assess the accumulated fatigue damage caused by TC winds. Each component is elaborated on in the following sections.

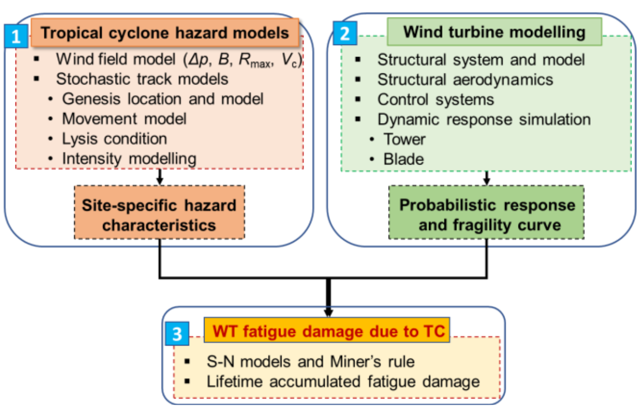

Figure 1: Diagram of the framework for assessing WT fatigue damage due to TCs.

2.2. TC hazard models

A stochastic autoregressive (AT) type of track model for landfalling TCs affecting mainland China (Li and Hong 2016) is adopted in the present study for simulating TC tracks. This model was developed based on the best TC track database from the China Meteorological Administration (CMA) (i.e., Shanghai typhoon center) and the parametric modeling approach advanced by Vickery et al. (2000). Given the information of a simulated TC track, the TC wind field model, known as the slab model (Vickery et al. 2000; Li and Hong 2015) is adopted to evaluate the TC wind field. The steps for simulating the surface TC wind speed affecting a site of interest are illustrated in Figure 2.

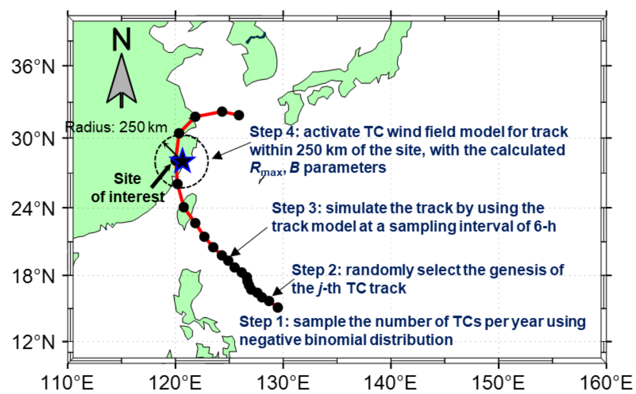

Figure 2: Illustration of steps for simulating TC track and calculating TC wind speed affecting a site of interest for a simulated track.

More specifically, the steps for generating samples of TC wind speed at a site of interest by considering a period of TC activities of T_T year (e.g., T_T = 100,000 years) are:

1) Sample the number of TCs for each year according to the developed probability distribution of the occurrence process (i.e., negative binomial distribution with parameters estimated from the best track dataset given by CMA (Li and Hong 2016; Sheng and Hong 2022). This results in a total of N_T number of tracks during T_T years;
2) Randomly select the genesis for the j-th TC track from the historical best track dataset given by CMA;
3) Sample the track with a sampling interval of 6 hrs by using the obtained genesis obtained in Step 2) and the adopted TC track model. Note that the points on the simulated track with a 6-hrs increment are used as the basis for

interpolation to obtain the track points with a 10-min increment.

4) Model the TC wind speed with the TC center on the TC track (i.e., points defined by 10-min increment)) that is within 250 km of the site of interest, where the needed parameters for the wind field model are those corresponding to the considered TC center. These parameters are determined based on the central pressure difference, Δ_p, and the filling-rate model (Li and Hong 2016). The radius to the maximum wind speed R_{max}, and Holland B parameter can be determined based on Δ_p (Vickery and Wadhera 2008). The obtained wind speed, donated as V_s, represents the 10-min mean TC wind speed at 10-m height.

2.3. WT model and dynamic response analysis

The second component shown in Figure 1 describes the development of the fragility curve based on structural analysis of the considered WT. The fragility curve is developed conditioned on V_s. Since, in general, an operating wind turbine is proprietary and its detailed information, including blades and the operating software, is unavailable, the NREL 5MW onshore WT is considered in the present study. This turbine is a three-blade horizontal axis WT with a hub height of 90 m. Parameters and settings for the considered WT is archived in the downloadable FAST (Fatigue, Aerodynamics, Structures, and Turbulence) software (Jonkman and Buhl 2005; Jonkman et al. 2009). The considered WT model is illustrated in Figure 3. The fully-coupled multi-body FEM of the considered WT is built in the FAST package. The dynamic time history analyses for the considered WT are carried out and the results are used to establish the database for the structural responses. For the analysis, we consider the Kaimal wind spectrum, exponential coherence model, power law wind profile with an exponent of 0.11, and turbulence intensity of 0.14 for Class B in operation and 0.11 for extreme wind conditions that are recommended in IEC 61400-1 (2019). The three-dimensional wind speed time histories are generated by using Turbsim, which is available in FAST (Jonkman 2006).

An illustration of the simulated 10-min wind speed time histories at hub height for V_s = 35 m/s

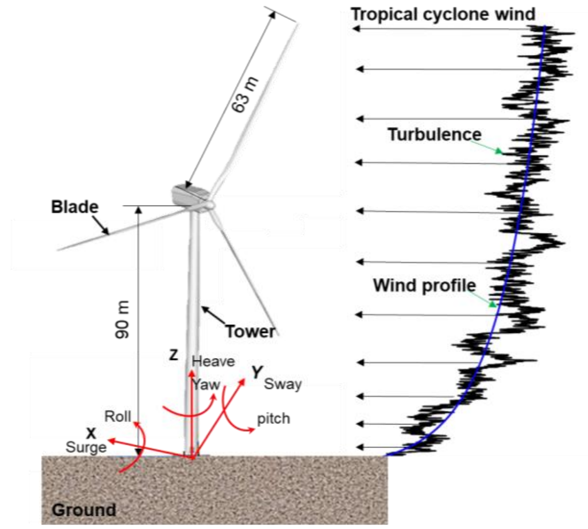

Figure 3: Schematic illustration of the NREL 5MW onshore WT subjected to TC wind.

is shown in Figure 4. It shows that the along-wind (i.e., X-direction) is fluctuating around a mean wind speed of 44.6 m/s at the hub height and the Y-direction wind is fluctuating around zero.

The response time histories for the tower and blade and the stress range and counted cycles for the simulated wind field shown in Figures 4a and 4b were presented in Figures 4c to 4f. Results in Figures 4c to 4d show the flapwise stress time history for the blade root and fore-aft stress time history for the tower base, respectively.

The plots shown in Figures 4e and 4f are to be discussed later.

2.4. Fatigue damage and S-N curve

The third component of the proposed framework is to evaluate WT fatigue damage accumulation by using the S-N curve. The simple S-N model combined with Miner's accumulation rule is widely employed in practice and making design code for WTs (DNV 2004; Márquez-Domínguez and Sørensen 2012).

For the WT steel tower, a bilinear S-N curve is often used. This curve is defined by,

$$\begin{cases} N_i = C_{d_1} / (\Delta\sigma_i)^{m_1}, N_i \le 10^7 \\ N_i = C_{d_2} / (\Delta\sigma_i)^{m_2}, N_i > 10^7 \end{cases}, \tag{1}$$

where N_i is the number of cycles to failure at the stress range $\Delta\sigma_i$; C_d (with an additional subscript 1 and 2) is the intercept of the S-N curve; m_1 and m_2 are the slopes of the S-N curve. The possible amplification factor to account for stress concentration and the effect of wall thickness are neglected. m_1 = 3, m_2 = 5, C_{d_1} = 11.546, and C_{d_2} = 14.576 (Chen et al. 2022) are adopted for the numerical analysis in the following. The bilinear S-N model is illustrated in Figure 5a.

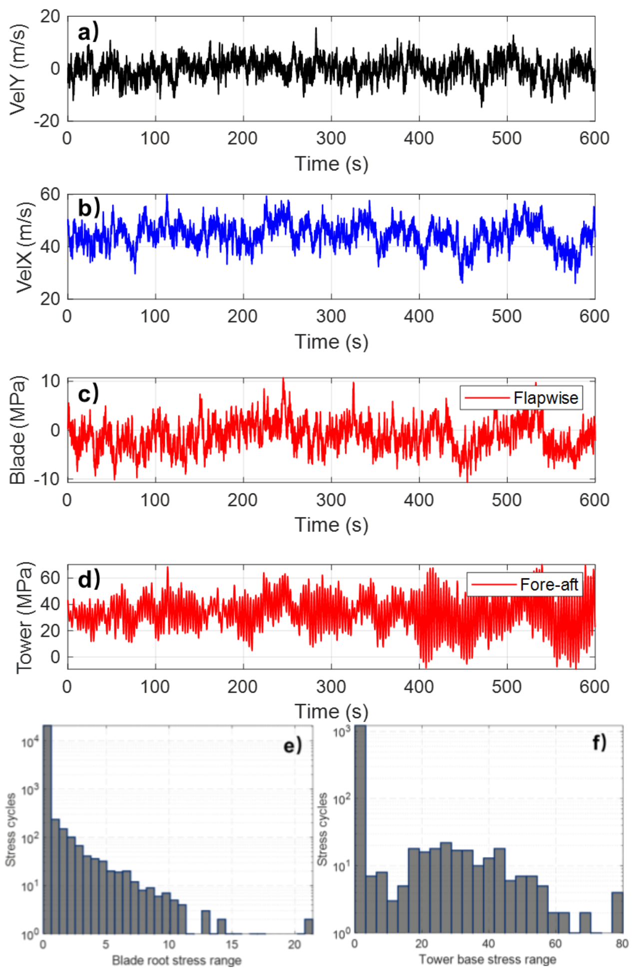

Figure 4: An illustration of simulated wind speed time histories for V_s = 35 m/s, the calculated structural dynamic response, and the histogram of stress range and cycles. a) Y-direction (across-wind) at hub height, b) X-direction (along-wind) at hub height, c) blade root flapwise stress in MPa, d) tower base fore-aft stress in MPa, e) histogram of the stress cycle for the blade root, and f) histogram of the stress cycle for the tower base.

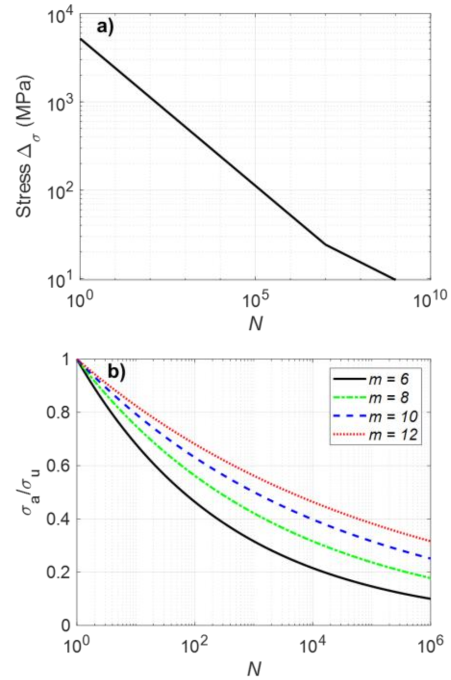

Figure 5: The adopted S-N models. a) for the tower and b) for the blade.

The WT blade is constructed using composite materials, such as fiberglass-reinforced polyester or epoxy, and with different manufacturing processes and technics. For such type of material, it is suggested that (Freebury and Musial 2000; Amirinia and Jung 2017),

$$\sigma_a = \sigma_u N^{-1/m}, \tag{2}$$

where σ_a and σ_u are the stress amplitude and ultimate stress amplitude, respectively. The parameter m typically ranges between 6 to 12 (Freebury and Musial 2000). An illustration of the S-N curves considering several m values is shown in Figure 5b. σ_u = 518 MPa and m = 6 are adopted in the present study.

The fatigue damage for 10 minutes duration wind with a specified mean wind speed, $D_{10-\min}$, can be estimated using the time histories of the structural responses obtained from FAST. It is calculated by using,

$$D_{10-\min} = \sum_{i}^{I} \frac{n_i}{N_i} = \frac{1}{C_d} \sum_{i}^{I} n_i \cdot (\Delta\sigma_i)^m \,, \tag{3}$$

where I is the total number of considered bins for the stress amplitudes. n_i is the stress cycle experienced by the structure for the corresponding stress amplitude $\Delta\sigma_i$. [C_d, m] equals [C_{d1}, m_1] for $N_i \leq 10^7$ and [C_{d2}, m_2] for $N_i > 10^7$.

Using the response time histories shown in Figures 4c and 4d, the histogram of the stress range is calculated and shown in Figures 4e to 4f. The figures show that the stress range for the tower is larger than that for the blade and the distributions of the stress range for the considered cases have different shapes.

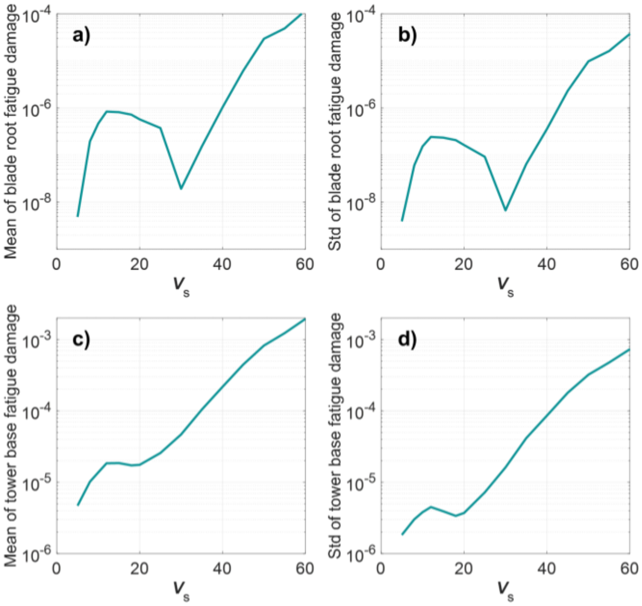

Figure 6: Statistics of accumulated fatigue damage for the considered WT obtained from the responses from FAST. (a) mean for the blade root, (b) std for the blade root, (c) mean for the tower base, and (d) std for the tower base.

To establish the fatigue damage database to be used to evaluate the accumulated lifetime fatigue damage, a set of V_s values ranging from 0 to 60 m/s are considered. For each wind speed, 100 runs of the dynamic time history analysis with a duration of 630 s are carried out (30 s was employed as the burn-in period). The rain-flow counting algorithm (ASTM 2017) is applied to the time history responses for the components of interest, such as the tower base and blade root, to obtain the number of stress cycle and amplitude statistics. Figure 6 shows the obtained mean and standard deviation (std) of the fatigue damage of the blade root and tower base obtained for the considered WT. It shows that fatigue damage for the wind speed within the operation regime can also be important. This is especially the case for the blade, which is affected by the mechanical control schemes and algorithm. As wind speed increases beyond the cut-out wind speed (i.e. 25 m/s at the hub height), the fatigue damage increases as well. The results and the response database are used for evaluating the cumulated fatigue damage due to the effect of a single TC event, and due to the number of TC events during the design working life of the WT.

The cumulative fatigue damage due to a TC event, D_E, are calculated using,

$$D_E = \sum_{k}^{K} D_{10-\min,k} \,, \tag{4}$$

where k and K are the k-th and total number of the (points) segments for a single TC track within 250 km from the site of interest with an increment of 10-min. $D_{10-\min,k}$ is the fatigue damage for the k-th point of a duration of 10 minutes. The accumulated fatigue damage for a year, $D_{TC,1}$, and for the design working life (i.e., 20 years), $D_{TC,20}$, are calculated using,

$$\begin{cases} D_{TC,1} = \sum_{p}^{P} D_{E,p} \\ D_{TC,20} = \sum_{n}^{20} \sum_{p}^{P_n} D_{E,n,p} \end{cases} , \tag{5}$$

where p denotes the p-th TC event affecting the WT during one year, P is the total number of TC events in a year, P_n is the total number of TC events in the n-th year, n denotes the n-th year within the service life lifetime, $D_{E,p}$ denotes the accumulated fatigue damage for the p-th event, and $D_{E,n,p}$ denotes the accumulated fatigue damage for the p-th event in the n-th year.

3. CASE STUDY FOR ONSHORE SITES ALONG THE SOUTHEAST COASTAL

REGION OF MAINLAND CHINA

3.1. The considered onshore sites and wind hazard statistics

The application of the described framework is illustrated by considering the NREL 5 MW onshore WT that is placed at two onshore sites identified in Figure 7 in the coastal region of mainland China, which is prone to TC hazards.

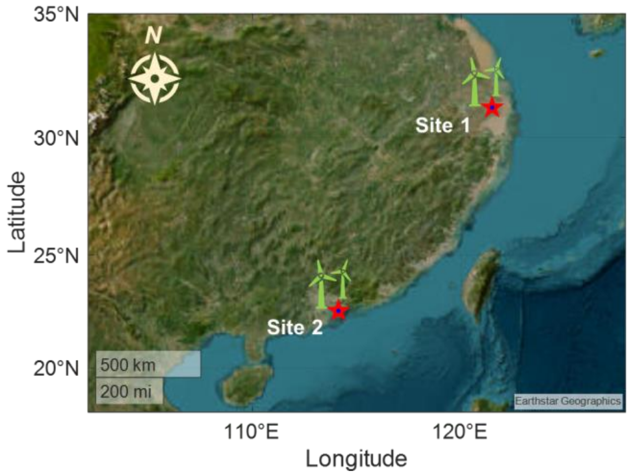

Figure 7: Two considered onshore sites in the southeast coastal region of mainland China.

By applying the TC hazard analysis explained earlier, the obtained samples of TC wind speed at the site of interest are employed for the extreme value analysis. The obtained T-year return period value of the annual maximum TC wind speed, $V_{\mathrm{a,max}}$, denoted as V_T, is shown in Table 1. For the analysis, 100,000 years of TC activities are simulated and considered.

Results in Table 1 indicate that the coefficient of variation (COV) of $V_{\mathrm{a,max}}$ is site-dependent. The value of COV is similar to that considered by Tarp-Johansen and Clausen (2006) for WT situated in the Philippines, but larger than about 0.135 that is found for synoptic winds (Hong et al. 2014; Mo et al. 2022). The estimated V_{50} for the considered sites is less than the 10-min mean wind speed at 10 height of 44.8 m/s, which corresponds to the TC design reference wind speed with a return period of 50 years stipulated in IEC 61400-1 (2019) (i.e., 10-min mean wind speed at hub height V_{hub} of 57 m/s). These values are also less than 43.2 m/s (i.e., V_{hub} = 55 m/s), which is the recommended design wind speed for Class TI system in GB/T 31519 (2015). It is interesting to note that 43.2 is larger and close to the V_{1000} for Site 1 and Site 2, respectively. This indicates that the referred design wind speed in IEC can be very conservative for the considered sites, although it is noted that IEC 61400-1 (2019) indicated that such a value is not necessarily applicable to all the sites in a TC hazard-prone region.

Table 1: The statistics of annual maximum wind speed $V_{a,max}$ and 50-, 100-, 500-, and 1000-year return period value of the annual maximum wind speed for the two considered sites.

Site	Mean (m/s)	COV	V_{50} (m/s)	V_{100} (m/s)	V_{500} (m/s)	V_{1000} (m/s)
# 1	10.1	0.80	28.1	30.9	37.0	39.7
# 2	16.8	0.46	34.1	36.6	41.4	43.2

3.2. Probabilistic characteristics of annual and lifetime accumulated fatigue damage

The distribution of the accumulated fatigue damage per year $D_{TC,1}$ for the two considered sites for the blade and tower is shown in Figure 8. The mean and COV of $D_{TC,1}$ are presented in Table 2. Results indicate that fatigue damage for different structural components differ and the fatigue damage for the tower base is much more severe as compared to that for the blade. The accumulated fatigue damage for the WT located at Site 2 is greater than that located at Site 1, reflecting the spatially varying TC wind hazard caused mainly by the spatially varying TC activities.

By considering 20 years of design service life, the samples and statistics of $D_{\mathrm{TC,20}}$ are computed and shown in Figure 9 and Table 2. The observed trends from Figure 9 are consistent with those observed in Figure 8. It is worth noting that if the fatigue design capacity based on Miner's rule is assumed to be equal to one, the TC-induced accumulated fatigue damage for the blade is 0.085% for Site 1 and 0.25% for Site 2, which are neglectable. However, these values for the tower base become 2.85% for Site 1 and 8.91 % for Site 2, respectively. The 8.91% reduction in capacity to sustain fatigue damage could be important for the design of the WT when considering TC. It is expected that a larger reduction of the capacity to sustain accumulated fatigue damage occurs if the WT is designed for V_{50} for the considered sites. The evaluation of this reduction for a WT that is specifically designed for the site based on the ultimate limit state is beyond the scope of the present study.

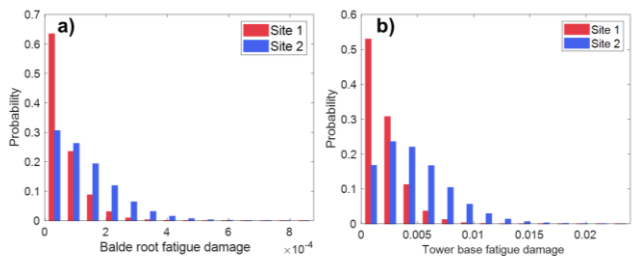

Figure 8: Histogram of accumulated fatigue damage per year by considering two geographic sites.

Table 2: Estimated annual and lifetime accumulated fatigue damage for two considered sites and WT.

Site	$D_{TC,1}$				$D_{TC,20}$			
	Blade root		Tower base		Blade root		Tower base	
	Mean	COV	Mean	COV	Mean	COV	Mean	COV
1	4.25×10^{-5}	5.80×10^{-5}	1.43×10^{-3}	1.64×10^{-3}	8.51×10^{-4}	2.64×10^{-4}	2.85×10^{-2}	7.55×10^{-3}
2	1.23×10^{-4}	1.04×10^{-4}	4.46×10^{-3}	3.10×10^{-3}	2.46×10^{-3}	4.55×10^{-4}	8.91×10^{-2}	1.36×10^{-2}

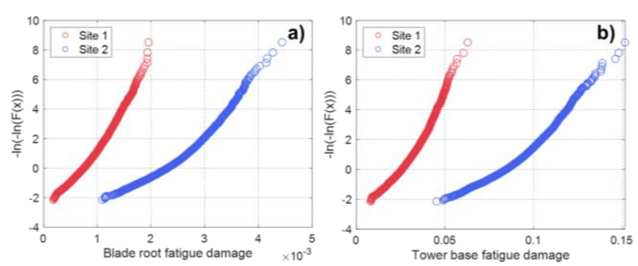

Figure 9: Empirical cumulative distribution function of accumulated fatigue damage during design life (plots are shown on Gumbel probability paper).

4. CONCLUSIONS

This study is focused on the framework for and illustration of the assessment of the accumulated fatigue damage for onshore wind turbines (WTs) subjected to tropical cyclone (TC) wind hazard. An overall framework is assembled which consists of sampling the TC tracks, evaluating the TC wind field based on the given track information, and calculating the responses of WT subjected to TC wind hazard using a fully-coupled multi-body finite element model (FEM).

Based on the considered framework, numerical analysis is carried out to evaluate the fatigue damage by considering the NREL 5MW onshore WT placed at two selected sites in the southeast coastal region of mainland China. The statistics of annual maximum wind speeds and the return period values of annual maximum TC wind hazards are evaluated. Furthermore, the accumulated fatigue damage per year and design working life is calculated. Results show that fatigue damage varies from site to site significantly. This can be explained by noting that TC hazard is geographically varying. The results also indicate that the fatigue damage for the tower can be more severe than that for the blade for the considered WT. For the considered case, the consideration of TC wind hazard could reduce the capacity for fatigue damage by about 9%. This observed reduction should be further scrutinized by considering the actual designed WT for the considered sites. The implication of such reduction should also be investigated in the context of developing design codes for WTs located in coastal regions that are prone to TC wind hazards.

5. ACKNOWLEDGMENTS

The financial support received from the Natural Sciences and Engineering Research Council of Canada, and the University of Western Ontario is gratefully acknowledged.

6. REFERENCES

Amirinia, G., & Jung, S. (2017). Buffeting response analysis of offshore wind turbines subjected to hurricanes. *Ocean Engineering*, 141, 1-11.

ASTM E1049-85 (2017), Standard Practices for Cycle Counting in Fatigue Analysis West Conshohocken, PA: *ASTM International*, 2011.

Chen, X., Li, C., & Xu, J. (2015). Failure investigation on a coastal wind farm damaged by super typhoon: A forensic engineering study. *Journal of Wind Engineering and Industrial Aerodynamics*, 147, 132-142.

Chen, Y., Wu, D., Yu, Y., & Gao, W. (2021). Do cyclone impacts really matter for the long-term performance of an offshore wind turbine?. *Renewable Energy*, 178, 184-201.

Chen, Y., Wu, D., Li, H., & Gao, W. (2022). Quantifying the Fatigue Life of Wind Turbines in Cyclone-Prone Regions. *Applied Mathematical Modelling*, 110, 455-474.

Clausen, N. E., Ott, S., Tarp-Johansen, N. J., Nørgard, P., Larsén, X. G., Pagalilawan, E. M., & Hernando, S. D. (2006). Design of wind turbines in an area with tropical cyclones. *European Wind Energy Conference and Exhibition*, Athens.

DNV (2004). Design of Offshore Wind Turbine Structure. *Offshore Standard* DNV-OS-J101.

Freebury, G., & Musial, W. (2000, January). Determining equivalent damage loading for full-scale wind turbine blade fatigue tests. *In 2000 ASME wind energy symposium*.

GB/T 31519-2015. (2015). Wind turbine generator system under typhoon condition, *Standards Press of China*, Beijing, China. (in Chinese).

Hallowell, S. T., Myers, A. T., Arwade, S. R., Pang, W., Rawal, P., Hines, E. M., ... & Fontana, C. M. (2018). Hurricane risk assessment of offshore wind turbines. *Renewable Energy*, 125, 234-249.

Hong, H. P., Mara, T. G., Morris, R., Li, S. H., & Ye, W. (2014). Basis for recommending an update of wind velocity pressures in Canadian design codes. *Canadian Journal of Civil Engineering*, 41(3), 206-221.

Hong, H.P., & Sheng C. (2022) Reliability-based calibration of site-specific design typhoon wind and wave loads for wind turbine, *Engineering Structures*, 270, 114885.

IEC International Electrotechnical Commission. IEC 61400-1: Wind turbines part 1:Design requirements. *International Electrotechnical Commission*; 2019.

Jonkman, B. J. (2006). TurbSim user's guide (No. NREL/TP-500-39797). *National Renewable Energy Laboratory*, Golden, CO (United States).

Jonkman, J. M., & Buhl, M. L. (2005). FAST user's guide (Vol. 365, p. 366). Golden, CO, USA: *National Renewable Energy Laboratory*, Golden, CO (United States).

Jonkman, J., Butterfield, S., Musial, W., & Scott, G. (2009). Definition of a 5-MW reference wind turbine for offshore system development (No. NREL/TP-500-38060). *National Renewable Energy Laboratory*, Golden, CO (United States).

Li, S. H., & Hong, H. P. (2015). Observations on a hurricane wind hazard model used to map extreme hurricane wind speed. *Journal of Structural Engineering*, 141(10), 04014238.

Li, S. H., & Hong, H. P. (2016). Typhoon wind hazard estimation for China using an empirical track model. *Natural Hazards*, 82(2), 1009-1029.

Li, Z. Q., Chen, S. J., Ma, H., & Feng, T. (2013). Design defect of wind turbine operating in typhoon activity zone. *Engineering Failure Analysis*, 27, 165-172.

Márquez-Domínguez, S., & Sørensen, J. D. (2012). Fatigue reliability and calibration of fatigue design factors for offshore wind turbines. *Energies*, 5(6), 1816-1834.

Mo, H. M., Hong, H. P., Li, S. H., & Fan, F. (2022). Impact of Annual Maximum Wind Speed in Mixed Wind Climates on Wind Hazard for Mainland China. *Natural Hazards Review*, 23(1), 04021061.

Rose, S., Jaramillo, P., Small, M. J., Grossmann, I., & Apt, J. (2012). Quantifying the hurricane risk to offshore wind turbines. *Proceedings of the National Academy of Sciences*, 109(9), 3247-3252.

Sheng, C., & Hong, H. P. (2020). On the joint tropical cyclone wind and wave hazard. *Structural Safety*, 84, 101917.

Sheng, C., & Hong, H. P. (2021). Reliability and fragility assessment of offshore floating wind turbine subjected to tropical cyclone hazard. *Structural Safety*, 93, 102138.

Sheng, C., & Hong, H. P. (2022). Sensitivity of typhoon wind hazard in coastal region to the track modelling and the considered historical best track database. *Journal of Wind Engineering and Industrial Aerodynamics*, 226, 105000.

Vickery, P. J., & Wadhera, D. (2008). Statistical models of Holland pressure profile parameter and radius to maximum winds of hurricanes from flight-level pressure and H* Wind data. *Journal of Applied Meteorology and climatology*, 47(10), 2497-2517.

Vickery, P. J., Skerlj, P. F., Steckley, A. C., & Twisdale, L. A. (2000). Hurricane wind field model for use in hurricane simulations. *Journal of Structural Engineering*, 126(10), 1203-1221.